






Cite this: *Green Chem.*, 2026, **28**, 5869

## A comparative study on heterogeneous CeO<sub>2</sub> and homogeneous 1,8-diazabicyclo[5.4.0]-7-undecene catalysts for conversion of CO<sub>2</sub> and monoethanolamine/ethylenediamine into cyclic compounds

Hiroki Sato,<sup>a</sup> Mizuho Yabushita,<sup>a</sup>  \*<sup>a</sup> Yingai Li,<sup>a</sup> Yoshinao Nakagawa <sup>a</sup> and Keiichi Tomishige  \*<sup>a,b</sup>

Heterogeneous CeO<sub>2</sub> and homogeneous 1,8-diazabicyclo[5.4.0]-7-undecene (DBU) catalysts have been employed for non-reductive conversion of CO<sub>2</sub>; however, their activity and catalysis have not yet been clarified clearly in identical reactions or conditions. Here, we conducted a kinetic study on the reactions between CO<sub>2</sub> and monoethanolamine (MEA) (or ethylenediamine (EDA)) producing 2-oxazolidinone (or 2-imidazolidinone) with the two catalysts under high CO<sub>2</sub>-pressure conditions. The conversion of MEA with CeO<sub>2</sub> proceeded faster than that with DBU under all the conditions tested in this study owing to the better affinity between CeO<sub>2</sub> and the possible intermediate of CO<sub>2</sub>-captured MEA. In contrast, the conversion of EDA over CeO<sub>2</sub> became slower at higher CO<sub>2</sub> pressure, while the same reaction with DBU was accelerated and became faster than that with CeO<sub>2</sub> upon the increase of CO<sub>2</sub> pressure. These contrasting behaviors of CeO<sub>2</sub>- and DBU-catalyzed reactions with change in CO<sub>2</sub> pressure were rationalized by the different effects of gaseous CO<sub>2</sub> on the possible intermediate species. In the case of CeO<sub>2</sub>, excess CO<sub>2</sub> capped the reactive amino group of an EDA-derived intermediate chemisorbed on the CeO<sub>2</sub> surfaces, decreasing the nucleophilicity of this functional group for the cyclization reaction and lessening the reaction rate. Meanwhile, the DBU-catalyzed reactions under high pressure CO<sub>2</sub> enabled the formation of the zwitterionic pair of CO<sub>2</sub>-captured DBU and CO<sub>2</sub>-captured EDA species, and such a strong electrostatic interaction between these species led to better reaction progress compared to low CO<sub>2</sub>-pressure conditions.

Received 11th December 2025,  
Accepted 4th March 2026

DOI: 10.1039/d5gc06699a

rsc.li/greenchem

### Green foundation

1. The kinetic and comparable insights into both homogeneous DBU and heterogeneous CeO<sub>2</sub> catalysts in non-reductive transformation of CO<sub>2</sub> to directly synthesize cyclic organic carbamates and urea derivatives are precious guidelines for maximizing the efficiency of reaction systems.
2. The catalytic performance of DBU and CeO<sub>2</sub> has been shown *via* a detailed kinetic study to be drastically impacted by CO<sub>2</sub> pressure, positing the great importance of selecting appropriate catalysts in accordance with the operating CO<sub>2</sub> pressure.
3. Life cycle assessment and techno-economic analysis will bring remaining issues to improve the feasibility of each catalytic system under its corresponding optimum conditions into sharp relief. Such information should be helpful for further improvement of feasibility of each catalytic system.

## 1. Introduction

Non-reductive conversion of carbon dioxide (CO<sub>2</sub>) has been recognized as a promising means of directly producing useful chemicals such as organic carbonates, organic carbamates,

and urea derivatives from CO<sub>2</sub> with alcohols and/or amines.<sup>1–9</sup> The non-toxic and non-flammable nature of CO<sub>2</sub> makes this means advantageous over conventional approaches for synthesizing such functional compounds that use hazardous carbonyl sources such as phosgene and carbon monoxide<sup>10–12</sup> from a safety perspective. Yet, there are two well-known obstacles in most of the non-reductive CO<sub>2</sub> conversion processes—severe thermodynamic limitation and low reactivity of CO<sub>2</sub>. For the former thermodynamic constraints, direct reactions of CO<sub>2</sub> with aliphatic/aromatic alcohols into organic carbonates are highly endergonic and thus suffer from quite low equilibrium

<sup>a</sup>Department of Applied Chemistry, Graduate School of Engineering, Tohoku University, 6-6-07 Aoba, Aramaki, Aoba-ku, Sendai, Miyagi 980-8579, Japan.

E-mail: m.yabushita@tohoku.ac.jp, tomishige@tohoku.ac.jp

<sup>b</sup>Advanced Institute for Materials Research (WPI-AIMR), Tohoku University, 2-1-1 Katahira, Aoba-ku, Sendai, Miyagi 980-8577, Japan

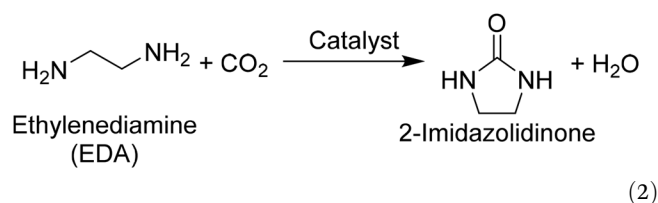
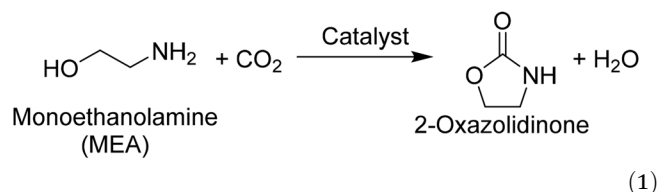


yields of target products (at most a few percent),<sup>1,4,12–14</sup> and such a severe equilibrium limitation can be overcome by removing co-produced water *via* dehydrating agents<sup>1,4,12–15</sup> and a gas stripping technique.<sup>16,17</sup> Meanwhile, equilibrium limitation is generally not severe in the production of organic urea derivatives from CO<sub>2</sub> and aliphatic amines owing to the high nucleophilicity of such amines, and high-yielding production of target compounds is possible without any dehydration technique.<sup>7</sup> For the latter obstacle of low reactivity of CO<sub>2</sub>, this gaseous compound needs to be activated with catalysts for rapid syntheses of the aforementioned useful chemicals, in contrast to the conventional phosgene method that proceeds well without catalysts.

Both heterogeneous and homogeneous catalysts have been reported to accelerate the non-reductive CO<sub>2</sub> conversion with other reactants (*e.g.*, alcohols and/or amines) thus far. Among various heterogeneous catalysts reported, CeO<sub>2</sub>-based materials have been shown to exhibit excellent catalytic activity because of their acid–base bifunctionality,<sup>9,18–34</sup> and exemplified reactions are listed in Table S1. Meanwhile, an organic and strongly basic compound, 1,8-diazabicyclo[5.4.0]-7-undecene (hereafter, abbreviated as DBU), was employed as one of the typical homogeneous catalysts for the non-reductive CO<sub>2</sub> conversion to produce cyclic carbamates from alkanolamines (Table S1),<sup>35,36</sup> urea from ammonia,<sup>37</sup> and polyureas from aliphatic diamines.<sup>38</sup> Due to the strongly basic nature originating from the amidine moiety, DBU chemically captures and activates CO<sub>2</sub>, which undergoes intermolecular reactions with ammonia and aliphatic amines. A DBU-immobilized catalyst was also developed for the two-step synthesis of organic carbamates from CO<sub>2</sub>, aliphatic amines, and alkyl halides, the latter of which were added to reaction mixtures after certain times.<sup>39</sup> DBU has also served as a catalyst for activating CO<sub>2</sub> to trigger cycloaddition with epoxides into cyclic carbonates,<sup>40–42</sup> polymerization with diamine into polyurea,<sup>43</sup> and carboxylative coupling with propargyl chlorides and primary aliphatic amines into organic carbamates.<sup>42</sup> In addition, the adduct of DBU and CO<sub>2</sub> was used for synthesizing organic carbamates<sup>44</sup> and urea derivatives,<sup>45</sup> and DBU-derived salts worked as catalysts in cycloaddition of CO<sub>2</sub> with epoxides.<sup>46</sup> These previous reports posit DBU to be the key homogeneous catalyst/mediator for converting CO<sub>2</sub> into value-added chemicals.

As alluded to above, both CeO<sub>2</sub> and DBU have been employed as a heterogeneous and homogeneous catalyst, respectively, not only in the production of organic carbamates directly from CO<sub>2</sub>, amines, and alcohols but also in other reactions including CO<sub>2</sub> as a reactant. From a practical perspective, CeO<sub>2</sub> is advantageous over DBU because of the ease of separation and reuse as well as the applicability to continuous-flow reactions. Meanwhile, from academic viewpoints such as kinetic and mechanistic studies, it remains unclear whether CeO<sub>2</sub> has further advantages beyond the general merits as a heterogeneous catalyst. The reason for this remaining issue is a lack of comparable reaction results acquired in the presence of CeO<sub>2</sub> and DBU for the same substrates under identical conditions, as seen in Table S1.

Therefore, in this study, such a comparative study was targeted with CeO<sub>2</sub> and DBU to reveal the characteristics of each catalyst. Considering that the presence of three reactants (*i.e.*, CO<sub>2</sub>, amine, and alcohol) with either catalyst in the production of organic carbamates makes the understanding of each reaction difficult, a single molecule possessing two terminal functional groups—2-aminoethanol (also called monoethanolamine (MEA))—was employed as a substrate to simplify the reaction system in this study. The target compound of this reaction is a cyclic organic carbamate, 2-oxazolidinone (eqn (1)). In addition, the structural analog of MEA, ethylenediamine (EDA), was also employed as a substrate to examine the catalysis of CeO<sub>2</sub> and DBU in the production of a cyclic urea derivative, 2-imidazolidinone (eqn (2)). For both reactions of MEA<sup>19,47</sup> and EDA<sup>48,49</sup> as well as their related substrates of CO<sub>2</sub>-captured amines (*i.e.*, alkylcarbamic acids),<sup>50–56</sup> CeO<sub>2</sub> was reported to exhibit higher catalytic activity compared to other metal oxides and afford good yields of 2-oxazolidinone and 2-imidazolidinone without dehydrating agents. Meanwhile, the absence of any catalyst failed to produce 2-oxazolidinone and 2-imidazolidinone from MEA + CO<sub>2</sub> (investigated at 423 K, 2 MPa of CO<sub>2</sub>)<sup>19</sup> and EDA + CO<sub>2</sub> (at 433 K, 0.5 MPa of CO<sub>2</sub>),<sup>48</sup> respectively. In addition, high CO<sub>2</sub> pressure was shown to decrease the rates of substrate conversion because of the capping of the terminal functional group (*i.e.*, hydroxy group for MEA and amino group for EDA) with excess CO<sub>2</sub>, while the maximum yield of target compounds was enhanced at higher CO<sub>2</sub> pressures due to the shift of equilibrium.<sup>19,48,57</sup>



We note that the non-reductive conversion of CO<sub>2</sub> with another structural analog of MEA, ethylene glycol, was not subject to this comparative study since this reaction suffers from severe reaction equilibrium (*e.g.*, the equilibrium yield of the target product (ethylene carbonate) was only 1.2% at 423 K),<sup>58</sup> and thus, the precise comparison between CeO<sub>2</sub> and DBU under the kinetic-controlled region is quite difficult. We also note that no dehydrating agent was employed in this study to fairly compare the activity and catalysis of CeO<sub>2</sub> and DBU due to the following two reasons. The first reason for no employment of dehydrating agents is given by a previously reported



fact that some dehydrating agents such as 2-cyanopyridine not only trigger equilibrium shift but also promote reactions *via* the generation of highly basic sites at the interface between CeO<sub>2</sub> and a chemisorbed 2-cyanopyridine molecule.<sup>59,60</sup> Such additional effects of dehydrating agents make the precise elucidation and comparison of catalytic activity between CeO<sub>2</sub> and DBU complicated or even impossible. Another reason originated from the not so severe equilibrium in the two target reactions operated in this study; indeed, over 80% yields of target products can be obtained even without dehydrating agents (exemplified data are shown later).

## 2. Experimental

### 2.1. Reagents

CeO<sub>2</sub> (HS grade) was purchased from Daiichi Kigenso Kagaku Kogyo and used after its calcination in air in an electric furnace at 873 K for 3 h, which were previously found as the optimum pretreatment conditions for the non-reductive conversion of CO<sub>2</sub> and amines (+alcohols) to produce urea derivatives (or organic carbamates).<sup>18,19,50,52,54</sup> Acetonitrile, ethylenediamine (EDA), and *tert*-butyl alcohol were obtained from FUJIFILM Wako Pure Chemical. 1,8-Diazabicyclo[5.4.0]-7-undecene (DBU), 2-aminoethanol (MEA), and D<sub>2</sub>O were obtained from Tokyo Chemical Industry.

### 2.2. Catalytic tests for the kinetic study

All the catalytic tests in this study were operated in a stainless-steel autoclave (HIRO Company, inner volume: 190 mL). Typically, 10 mmol of substrate, 1–5 mmol of either CeO<sub>2</sub> or DBU as a catalyst, 500 mmol of acetonitrile as a solvent, and a stirring bar were charged into the autoclave. After sealing, the autoclave was purged and pressured with Ar to 1 MPa at room temperature. The reactor was heated to the target temperature with magnetic stirring at 250 rpm. When the inner temperature of the reactor, which was monitored using a K-type thermocouple, reached the designated one, the autoclave was pressured with CO<sub>2</sub> to 2 MPa. This procedure for introducing CO<sub>2</sub> into the reactor at the target temperature enabled us to suppress the undesired reaction progress during the temperature-ramping process and acquire kinetic data precisely.<sup>61</sup> The time when the pressurization with CO<sub>2</sub> was completed was defined as 0 h of reaction time. After the reaction operation for a specific time, the autoclave was immersed in a water bath to be quickly cooled to room temperature. The reaction mixture was collected with distilled water and filtered using a polytetrafluoroethylene (PTFE) syringe filter (0.2 μm mesh). For all the reactions except for those with an MEA substrate, the liquid phase was analyzed using a gas chromatograph with a flame-ionization detector (GC-FID; Shimadzu, GC-2014) equipped with an InertCap for Amines capillary column (GL Sciences, Ø0.32 mm × 30 m). In the case of MEA, the liquid phase was mixed with D<sub>2</sub>O and *tert*-butyl alcohol, the latter of which was used as an internal standard and analyzed by <sup>1</sup>H nuclear magnetic resonance spectroscopy (<sup>1</sup>H NMR; Bruker,

AV400, superconducting magnet 9.4 T, <sup>1</sup>H 400 MHz). The <sup>1</sup>H NMR spectra of typical reaction mixtures as well as authentic samples are shown in Fig. S1–S8. The spent CeO<sub>2</sub> catalyst was employed for thermogravimetry and differential thermal analyses (TG-DTA; Thermo Plus EVOII, Rigaku); for the measurement, *ca.* 10 mg of the catalyst was heat-treated in an air flow (500 mL min<sup>-1</sup>) with a ramp rate of 10 K min<sup>-1</sup> from room temperature to 1173 K. The fresh and spent catalysts were analyzed by powder X-ray diffraction measurement (XRD; MiniFlex600, Rigaku, Cu Kα radiation at 40 kV and 40 mA) and scanning transmission electron microscopy (STEM; HD-2700, Hitachi).

## 3. Results and discussion

### 3.1. Comparison of CeO<sub>2</sub> and DBU in the conversion of MEA and CO<sub>2</sub>

The catalytic activity of CeO<sub>2</sub> and DBU was initially compared in the conversion of MEA and CO<sub>2</sub> (eqn (1)) at 403 K under various conditions. It should be noted that all the data in this study were acquired in the kinetic region to fairly compare the activity of the two catalysts by taking the difference of their activity into account; hence, such a difference made us employ each appropriate catalyst amount in order to adjust the reaction progress within the kinetically controlled level and compare their catalytic activity on the basis of reaction rate per catalyst amount. In this reaction, the CeO<sub>2</sub> catalyst was previously shown to exhibit good reusability in its four-time reuse after washing with methanol, drying at 383 K, and calcination in air at 873 K,<sup>19</sup> with the preservation of its structural properties as confirmed by XRD (Fig. S9) and STEM (Fig. S10); within this context, neither deactivation nor structural change of the CeO<sub>2</sub> catalyst needs to be considered in the kinetic study discussed below. We also note that the high-yielding production of the target product (*i.e.*, 2-oxazolidinone) was possible by using both CeO<sub>2</sub> and DBU catalysts (≥80%; Fig. S11A and Table S2). In these reactions for the high-yielding production of 2-oxazolidinone, the reactor was pressurized to 2 MPa with CO<sub>2</sub> at room temperature (*r.t.*) and then heated to 403 K. In stark contrast, all the kinetic data were acquired in this study with the more precise experimental procedure as we employed previously;<sup>61</sup> the reactor was initially heated to the desired temperatures and then pressurized with CO<sub>2</sub> to eliminate the contributions of reaction progress during temperature ramp.

As listed in Table 1 (the second data point from the right in Fig. 1A; detailed information is also available in Fig. S12 and Table S4), CeO<sub>2</sub> exhibited 0.80 mmol mmol<sub>cat</sub><sup>-1</sup> h<sup>-1</sup> formation rate of 2-oxazolidinone (entry 1), which is the target product in this reaction, in 380 mM MEA solution at 2 MPa of CO<sub>2</sub> pressure. This rate was 17-fold higher than that given by DBU (entry 2). Considering that the formation of 2-oxazolidinone proceeds on the surface of CeO<sub>2</sub> where 0.97 mmol g<sup>-1</sup> Ce atoms are calculated to be present (detailed calculation procedure is described in the SI), its formation rate based on the number of Ce atoms at the surface (*i.e.*, turnover frequency



**Table 1** Summary of the kinetic study on the conversion of MEA/EDA and CO<sub>2</sub> with the CeO<sub>2</sub> or DBU catalyst<sup>a</sup>

HOCH2CH2NH2 + CO2 >>[Catalyst, -H2O] O=C1NCCO1  
 MEA → 2-Oxazolidinone

H2NCH2CH2NH2 + CO2 >>[Catalyst, -H2O] O=C1NCCN1  
 EDA → 2-Imidazolidinone

Entry	Substrate	Product	Catalyst	Formation rate (403 K, CO <sub>2</sub> – 2 MPa) [mmol mmol <sup>-1</sup> h <sup>-1</sup> ]	Reaction order <sup>b</sup>		<i>E<sub>a</sub></i> <sup>c</sup> [kJ mol <sup>-1</sup> ]
					<i>P</i> (CO <sub>2</sub> )	Substrate conc.	
1	MEA	2-Oxazolidinone	CeO <sub>2</sub>	0.80	0.0	0.0	64
2			DBU	0.047	0.3	1.1	91
3	EDA	2-Imidazolidinone	CeO <sub>2</sub>	0.11 (0.54) <sup>d</sup>	-0.5	-0.2	117 (76) <sup>d</sup>
4			DBU	0.11	0.5	0.3	95

<sup>a</sup>The Arrhenius plots and double logarithmic plots for elucidation of the reaction order are depicted in Fig. 1–3, which are drawn on the basis of the reaction data summarized in Fig. S12–S14 and S16–S19 as well as Tables S4–S6 and S7–S10. <sup>b</sup>At 403 K. <sup>c</sup>Apparent activation energy at 2 MPa of CO<sub>2</sub> pressure. <sup>d</sup>The values in parentheses were determined at 0.2 MPa of CO<sub>2</sub> pressure.

(TOF) was estimated to be 5.9 mmol mmol<sub>Ce</sub><sup>-1</sup> h<sup>-1</sup>, which was 125-fold higher than that in the case of DBU. Likewise, even at the other reaction temperatures ranging from 393 K to 423 K (Fig. 1A and Fig. S12 and Table S4), higher formation rates of 2-oxazolidinone were given by CeO<sub>2</sub> rather than by DBU. These data clearly showed the higher catalytic activity of CeO<sub>2</sub> for this reaction compared to DBU within the whole temperature range in this study. This observed rank of catalytic activity between the two catalysts was also reflected by the lower apparent activation energy (*E<sub>a</sub>*) for CeO<sub>2</sub> (64 kJ mol<sup>-1</sup>) than that for DBU (91 kJ mol<sup>-1</sup>).

The reaction orders with respect to the CO<sub>2</sub> pressure and MEA concentration in the presence of either CeO<sub>2</sub> or DBU catalyst were then examined at 403 K by varying these parameters, as shown in Fig. 1B–E and Fig. S13 and S14 (detailed data are listed in Tables S5 and S6). Under all the conditions investigated here, the activity of the CeO<sub>2</sub> catalyst was superior to that of DBU. In the case of CeO<sub>2</sub>, zero-order dependence was observed for both CO<sub>2</sub> pressure and MEA concentration (entry 1 in Table 1 and Fig. 1B and D). Considering that amines readily capture CO<sub>2</sub> chemically as alkylcarbamic acids,<sup>62–64</sup> CO<sub>2</sub>-captured MEA (*i.e.*, (2-hydroxyethyl)carbamic acid; hereafter, denoted as MEA-CA) was assumed to be an intermediate in this reaction; indeed, related studies often reported alkylcarbamic acids as intermediates in the formation of urea derivatives from amines and CO<sub>2</sub>.<sup>48,65–68</sup> Besides, the catalytic transformation of MEA-CA in MEA solvent over CeO<sub>2</sub> was shown recently to produce a linear urea derivative *via* 2-oxazolidinone as an intermediate.<sup>56</sup> The observed zero-order dependence with respect to both CO<sub>2</sub> pressure and MEA concentration thus indicated that the surfaces of the CeO<sub>2</sub> catalyst were saturated by MEA-CA. In contrast, in the DBU-catalyzed conversion of MEA, the reaction orders with respect to the CO<sub>2</sub> pressure and MEA concentration were determined to be 0.3 and 1.1, respectively (entry 2 in Table 1 and Fig. 1C and E). These positive reaction orders indicated the weak interaction between DBU and MEA-CA. Due to the presence of excess CO<sub>2</sub> against MEA, the concentration of the plausible intermediate MEA-CA was dependent on the

amount of MEA, not on the CO<sub>2</sub> pressure. This fact could be connected to the observation of the larger positive reaction order with respect to MEA concentration compared to CO<sub>2</sub> pressure. Yet, the slightly positive reaction order with respect to CO<sub>2</sub> pressure still pointed to the importance of CO<sub>2</sub> in the gas phase for the reaction progress. Altogether, CeO<sub>2</sub> was superior to DBU as a catalyst in terms of the activity for the production of 2-oxazolidinone from MEA and CO<sub>2</sub> under all the reaction conditions ranging from low to high CO<sub>2</sub> pressure.

### 3.2. Comparison of CeO<sub>2</sub> and DBU in the conversion of EDA and CO<sub>2</sub>

The kinetic study on the conversion of EDA and CO<sub>2</sub> (eqn (2)) was performed with CeO<sub>2</sub> and DBU. We note that the yield of the target product (*i.e.*, 2-imidazolidinone) reached as high as 94% in the presence of the DBU catalyst; meanwhile, the reaction with CeO<sub>2</sub> became quite slow with a long reaction time, and the yield of 2-imidazolidinone was 45% even at 96 h (Fig. S11B and Table S3). This behavior of CeO<sub>2</sub> was due to the catalyst deactivation by the surface deposition of organic species, as confirmed by the observation of weight decrease with exothermic peaks in TG-DTA (Fig. S15). Such catalyst deactivation was also found previously in the conversion of CO<sub>2</sub>-absorbed ethylenediamine (*i.e.*, (2-aminoethyl)carbamic acid, abbreviated as EDA-CA) in EDA solvent, where insoluble poly-urea-like compounds were accumulated on the catalyst surfaces and led to the deactivation.<sup>52</sup> The structural change of the CeO<sub>2</sub> catalyst was not the reason for such deactivation shown by no obvious difference in its XRD pattern (Fig. S9) and STEM image (Fig. S10). Furthermore, appropriate treatment consisting of washing with methanol, drying at 383 K, and calcination in air at 873 K was demonstrated in our former study to regenerate the catalytic activity of CeO<sub>2</sub>.<sup>48</sup> To avoid the underestimation of the catalytic activity of CeO<sub>2</sub> and enable a fair comparison between DBU and CeO<sub>2</sub> catalysts, the very initial stage of reaction time course was carefully examined in this study.



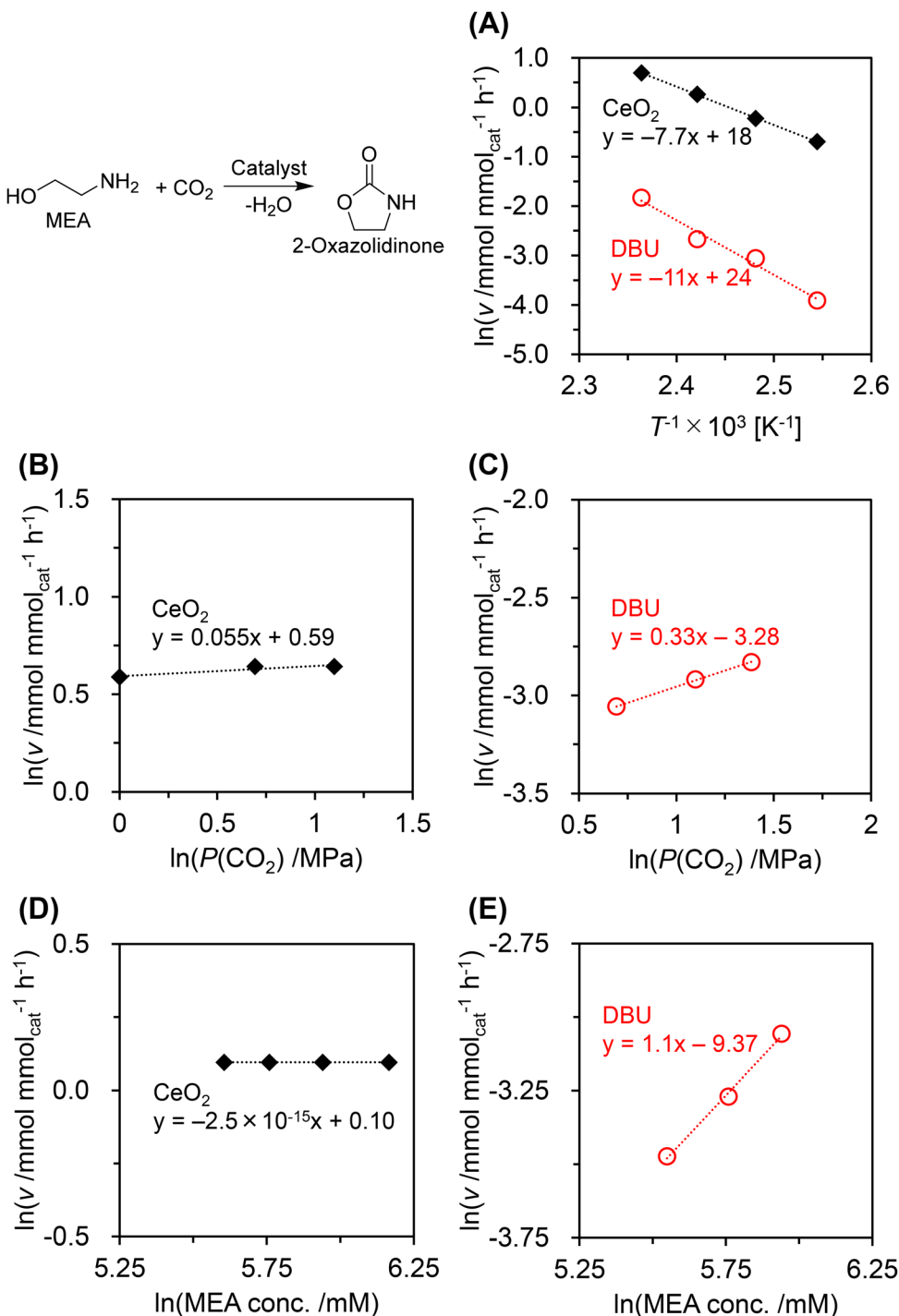
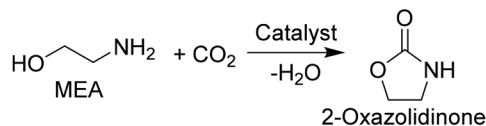


**Fig. 1** Comparison of CeO<sub>2</sub> and DBU catalysts in the conversion of MEA and CO<sub>2</sub>. (A) Arrhenius plot at 2 MPa of CO<sub>2</sub> pressure. Double logarithmic plot for the formation rate of 2-oxazolidinone versus partial pressure of CO<sub>2</sub> with (B) CeO<sub>2</sub> and (C) DBU at 403 K. Double logarithmic plot for the formation rate of 2-oxazolidinone versus the initial concentration of MEA with (D) CeO<sub>2</sub> and (E) DBU at 403 K. Detailed data are shown in Fig. S12–S14 and Tables S4–S6.

Akin to the aforementioned reaction of MEA and CO<sub>2</sub>, the activity of these catalysts was initially elucidated and compared in 380 mM EDA solution at 403 K at 2 MPa of CO<sub>2</sub> pressure (entries 3 and 4 in Table 1, the first data points from the right in Fig. 2A; detailed information is also available in Fig. S16 and Table S7). In this reaction, the formation rates of the

target product 2-imidazolidinone given by CeO<sub>2</sub> and DBU were both 0.11 mmol mmol<sub>cat</sub><sup>-1</sup> h<sup>-1</sup>, indicating similar mole-basis activity of these catalysts under the given conditions. On the basis of the surface Ce atoms (*vide supra*), the formation rate of 2-imidazolidinone over CeO<sub>2</sub> was calculated to be 0.81 mmol mmol<sub>Ce</sub><sup>-1</sup> h<sup>-1</sup>. At the higher temperatures of 413 K



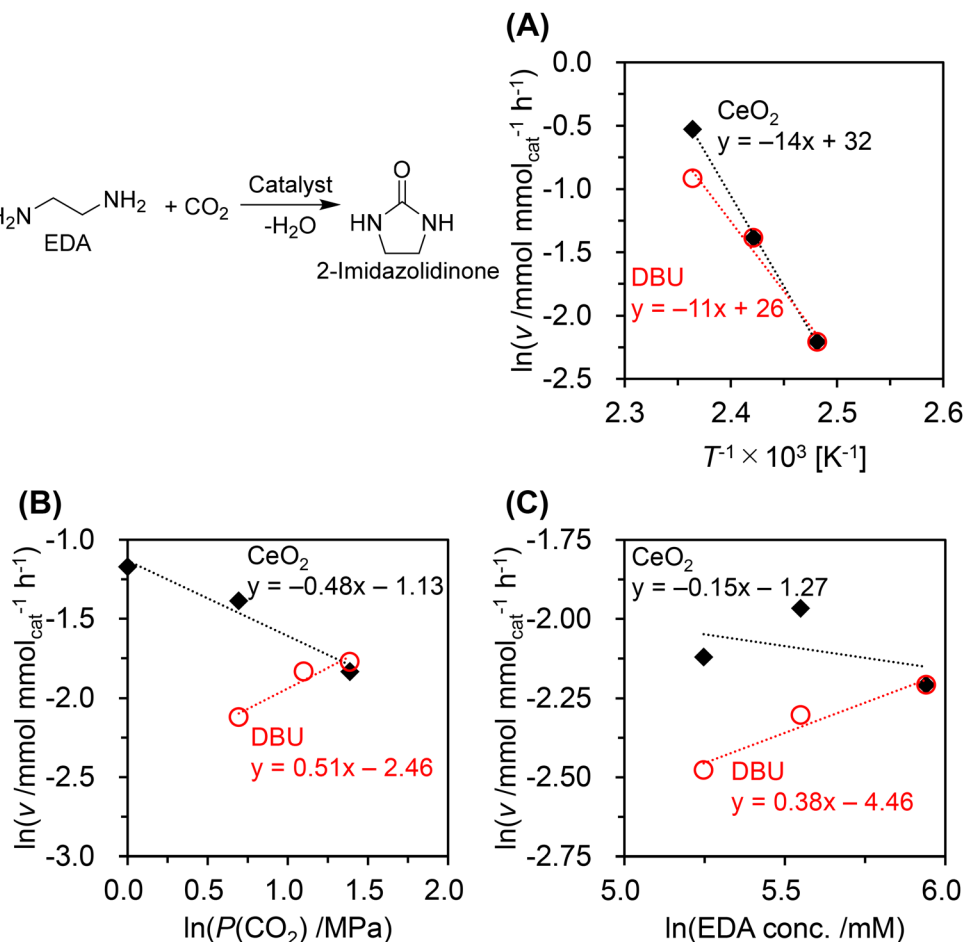
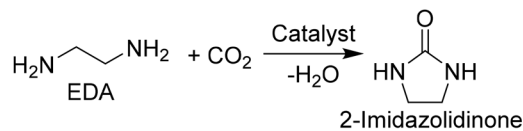


**Fig. 2** Comparison of  $\text{CeO}_2$  and DBU catalysts in the conversion of EDA and  $\text{CO}_2$ . (A) Arrhenius plot at 2 MPa of  $\text{CO}_2$  pressure. (B) Double logarithmic plot for the formation rate of 2-imidazolidinone versus partial pressure of  $\text{CO}_2$  with either  $\text{CeO}_2$  or DBU at 403 K. (C) Double logarithmic plot for the formation rate of 2-imidazolidinone versus the initial concentration of EDA with either  $\text{CeO}_2$  or DBU at 403 K. Detailed data are shown in Fig. S16, S17, and S19 as well as Tables S7, S8, and S10.

and 423 K, the formation of 2-imidazolidinone over  $\text{CeO}_2$  was faster than that over DBU (Fig. 2A). The negatively steeper slope for  $\text{CeO}_2$  in this Arrhenius plot provided a higher  $E_a$  of  $117 \text{ kJ mol}^{-1}$  (entry 3 in Table 1) relative to the  $95 \text{ kJ mol}^{-1}$  for DBU (entry 4). One of the possible factors for the high  $E_a$  value for  $\text{CeO}_2$  is its stronger affinity for EDA molecules that possess two basic amino groups due to its amphoteric nature, compared to basic DBU. This trend was opposite to that in the reaction between MEA and  $\text{CO}_2$  to produce 2-oxazolidinone with  $\text{CeO}_2$  and DBU (see section 3.1) and can be rationalized by the dependence of activity of  $\text{CeO}_2$  on  $\text{CO}_2$  pressure and the reaction mechanism. As seen in Fig. 2B, the negative reaction order with respect to  $\text{CO}_2$  pressure (*i.e.*,  $-0.5$ , entry 3 in Table 1; more detailed data are available in Fig. S17 and Table S8) was observed in the reaction between EDA and  $\text{CO}_2$  over  $\text{CeO}_2$ , indicating the inhibitory effect of  $\text{CO}_2$  in the gas phase. The double logarithmic plot in Fig. 2 clearly shows that the formation rate of 2-imidazolidinone over  $\text{CeO}_2$  became lower than that with DBU at high  $\text{CO}_2$  pressure. As proposed previously, the free amino group in the possible intermediate,

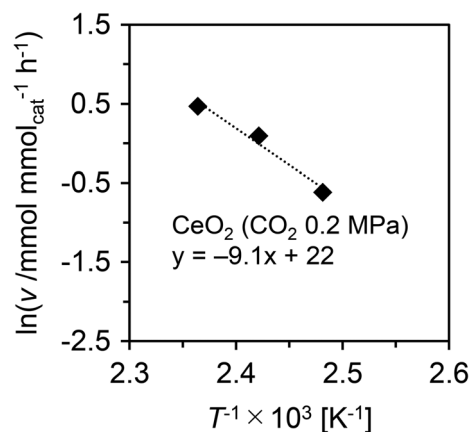


**Fig. 3** Arrhenius plot for the conversion of EDA and  $\text{CO}_2$  over the  $\text{CeO}_2$  catalyst at a  $\text{CO}_2$  pressure of 0.2 MPa (*i.e.*, equivalent to EDA). Detailed data are shown in Fig. S18 and Table S9.



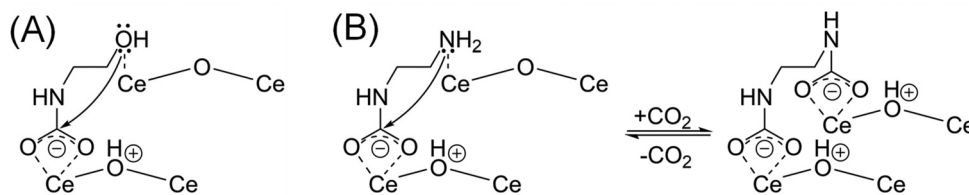


Fig. 4 Plausible differences between the cyclization of each substrate in the presence of excess  $\text{CO}_2$  over  $\text{CeO}_2$  catalyst: (A) MEA and (B) EDA.

$\text{CO}_2$ -absorbed EDA (*i.e.*, EDA-CA), chemisorbed on the surfaces of  $\text{CeO}_2$  is possibly capped with gaseous  $\text{CO}_2$  *via* an acid-base reaction in the presence of excess  $\text{CO}_2$ , resulting in the decrease of nucleophilicity of the amino group that is a prerequisite for the cyclization to form 2-imidazolidinone (detailed description and scheme are provided later).<sup>48,50,57</sup> Due to the requirement of the removal of such capping  $\text{CO}_2$ , the reactions with  $\text{CeO}_2$  had a relatively high  $E_a$ . Indeed, the  $E_a$  at a low  $\text{CO}_2$  pressure (*i.e.*, 0.2 MPa, which is equivalent to EDA (10 mmol)) was determined from the Arrhenius plot in Fig. 3 to be  $76 \text{ kJ mol}^{-1}$  (entry 3 in Table 1; more detailed data are available in Fig. S18 and Table S9), which was by  $41 \text{ kJ mol}^{-1}$  lower than that at 2 MPa of  $\text{CO}_2$  pressure. The formation rate of 2-imidazolidinone at 0.2 MPa of  $\text{CO}_2$  pressure was  $0.54 \text{ mmol mmol}_{\text{cat}}^{-1} \text{ h}^{-1}$ , which was closer to that of 2-oxazolidinone over the same catalyst (entry 1). These  $E_a$  values showed the significant inhibitory effect of excess  $\text{CO}_2$  on the  $\text{CeO}_2$ -catalyzed reaction of EDA. The reaction order with respect to EDA concentration determined from the raw data in Fig. S19 and Table S10 was  $-0.2$ , which was close to zero-order dependence and suggested the saturation of  $\text{CeO}_2$  surfaces with the above-mentioned intermediate, EDA-CA.

In stark contrast to the  $\text{CeO}_2$ -catalyzed conversion of EDA and  $\text{CO}_2$ , the reaction order with respect to  $\text{CO}_2$  pressure in the presence of the DBU catalyst was positively large (*i.e.*, 0.5, entry 4 in Table 1 and Fig. 2B; more detailed data are available in Fig. S17 and Table S8). The presence of excess  $\text{CO}_2$  was, therefore, preferable for the reaction progress and should offer the ease of formation of key intermediate species (detailed discussion is given later). Due to such dependence, as described above, the use of DBU as a catalyst was favorable over that of  $\text{CeO}_2$  in the conversion of EDA operated under high pressure  $\text{CO}_2$ . The reaction order with respect to EDA concentration was slightly positive (entry 4 in Table 1; more detailed reaction data are available in Fig. S19 and Table S10), indicating the relatively strong interaction between DBU and the plausible intermediate EDA-CA. Overall, the appropriate catalyst needs to be chosen for the production of 2-imidazolidinone from EDA and  $\text{CO}_2$  with consideration of  $\text{CO}_2$  pressure; that is, the desire to operate reactions at low  $\text{CO}_2$  pressure makes  $\text{CeO}_2$  a more suitable catalyst, while DBU is a preferable catalyst for reactions operated at high  $\text{CO}_2$  pressure.

### 3.3. The plausible reaction mechanism of the conversion of MEA/EDA and $\text{CO}_2$ in the presence of $\text{CeO}_2$ /DBU

On the basis of the aforementioned kinetic results for the conversion of MEA/EDA with  $\text{CO}_2$  in the presence of either  $\text{CeO}_2$

or DBU as a catalyst (Table 1), the reaction mechanisms for each reaction are proposed in this section. In the  $\text{CeO}_2$ -catalyzed reactions, the dependence on  $\text{CO}_2$  pressure was significantly different between the reaction of MEA (zero-order) and that of EDA (negative order). The former zero-order dependence with respect to  $\text{CO}_2$  pressure (and also the MEA concentration) can be explained by the saturation of  $\text{CeO}_2$  surfaces with the intermediate species that are readily produced from  $\text{CO}_2$  and MEA (*i.e.*, MEA-CA). On the  $\text{CeO}_2$  surfaces, such chemisorbed and activated MEA-CA underwent the intermolecular nucleophilic attack by the terminal hydroxy group toward the carbonyl carbon to form the cyclic compound 2-oxazolidinone (Fig. 4A). Due to the neutral nature of the hydroxy group, acidic  $\text{CO}_2$  in the gas phase does not influence the reactivity of this functional group, and therefore, the negative impact of  $\text{CO}_2$  was not observed in this reaction.

Even in the case of EDA conversion over  $\text{CeO}_2$ , the intermediate species EDA-CA, which is easily formed *via* chemical absorption of  $\text{CO}_2$  into EDA,<sup>50,51,69</sup> should readily interact with the  $\text{CeO}_2$  surfaces as reported previously.<sup>51,52</sup> Yet, the highly basic terminal amino group in this intermediate was problematic in the presence of excess  $\text{CO}_2$ . This functional group needs to attack the carbonyl carbon as illustrated in the left side of Fig. 4B for the cyclization to form 2-imidazolidinone; however, this amino group should readily react with gaseous  $\text{CO}_2$  *via* an acid-base reaction and lose its nucleophilicity (the right side of Fig. 4B), and the same rationale was provided in previous reports.<sup>48,50,57</sup> In other words, the activation of amino groups *via* the removal of capping  $\text{CO}_2$  is necessary for the production of 2-imidazolidinone. This discussion can also be rationalized by the higher  $E_a$  value at 2 MPa of  $\text{CO}_2$  pressure (*i.e.*, excess  $\text{CO}_2$  conditions) than that at 0.2 MPa (*i.e.*, equivalent  $\text{CO}_2$  conditions).

In the reactions catalyzed by DBU, the positive reaction orders with respect to  $\text{CO}_2$  pressure were observed to a greater or lesser extent, indicating the favorability of high  $\text{CO}_2$ -pressure conditions. According to previous studies, the chemical absorption of  $\text{CO}_2$  by a mixture of DBU and amine readily generated an ion pair of a protonated DBU cation and a carbamate anion.<sup>70–73</sup> In the same manner as these reports, such an ion pair was also formed initially in our reactions using DBU as a catalyst (see the first step in Fig. 5). Under the high  $\text{CO}_2$ -pressure conditions, another  $\text{CO}_2$  molecule was assumed to be captured at the DBU side along with the transfer of the proton from protonated DBU to the amino group in another MEA molecule in the MEA conversion (or the counter EDA-CA anion



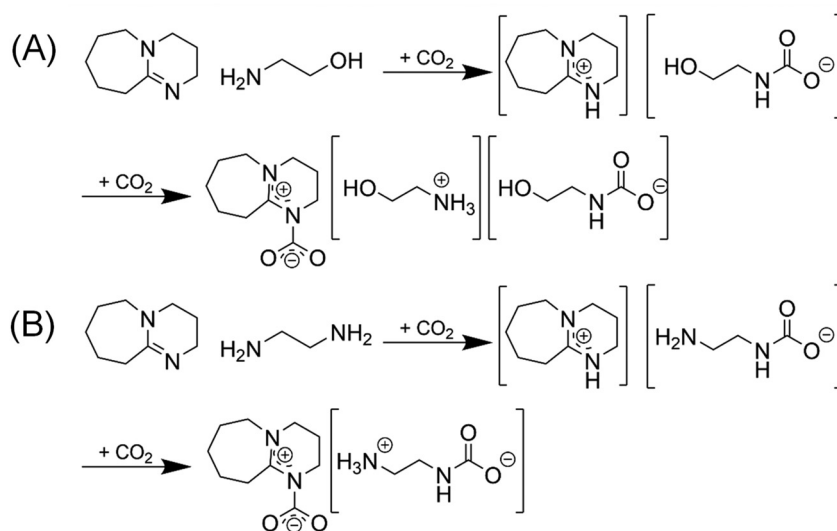


Fig. 5 Plausible ion pairs of DBU and each substrate in the presence of excess CO<sub>2</sub>: (A) MEA and (B) EDA.

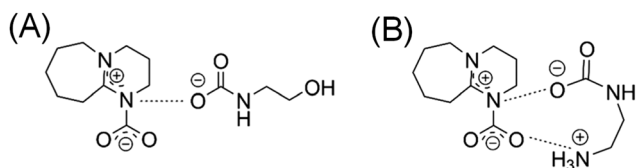


Fig. 6 Possible interaction between zwitterionic CO<sub>2</sub>-captured DBU and the (zwitter)ionic CO<sub>2</sub>-captured substrate: (A) MEA and (B) EDA.

in the EDA conversion), as shown in the second step in Fig. 5. Such capture of additional CO<sub>2</sub> molecule(s) in the presence of enough CO<sub>2</sub> was also reported for various CO<sub>2</sub>-capturing systems using sole amine or multiple amines, resulting in the formation of multivalent ionic species.<sup>74–78</sup> This step generated the zwitterionic DBU species possessing delocalized positive and negative charges at the amidine and captured CO<sub>2</sub> moieties, respectively. In the conversion of EDA, both DBU- and EDA-derived species were in the zwitterionic state, and two pairs of positive and negative charges led to a strong electrostatic interaction between these species (Fig. 6B). Meanwhile, in the conversion of MEA, due to the presence of single negative charge in the MEA-derived species, the electrostatic interaction between such species and DBU-derived zwitterionic species could be weak. The degree of interaction strength between DBU- and substrate-derived species was indeed reflected by the large difference between the reaction orders with respect to the concentration of each substrate (*i.e.*, 1.1 for MEA *versus* 0.3 for EDA; Table 1). The strong basic nature of DBU possibly enabled it to capture additional CO<sub>2</sub> and be beneficial for the operation of reactions (namely, EDA conversion) at high CO<sub>2</sub> pressure. In contrast, in the case of acid–base bifunctional CeO<sub>2</sub> whose basicity is weaker than amines, the highly basic amino moiety of chemisorbed

EDA-CA was capped with CO<sub>2</sub>, resulting in the negative impact of CO<sub>2</sub> pressure on the formation rate of 2-imidazolidinone.

## 4. Conclusions

This work compared the activity and catalysis of heterogeneous CeO<sub>2</sub> and homogeneous 1,8-diazabicyclo[5.4.0]-7-undecene (DBU) catalysts, both of which have been employed for various non-reductive CO<sub>2</sub> conversions thus far, in the two model reactions using either monoethanolamine (MEA) or ethylenediamine (EDA) as a substrate under high CO<sub>2</sub>-pressure conditions. In the former reaction, the activity of the CeO<sub>2</sub> catalyst was superior to that of DBU regardless of reaction temperature, CO<sub>2</sub> pressure, or MEA concentration. Meanwhile, the activity of DBU became higher than that of CeO<sub>2</sub> at high CO<sub>2</sub> pressure in the conversion of EDA because of the inhibitory effect of excess CO<sub>2</sub> on the CeO<sub>2</sub>-catalyzed EDA conversion. In the conversion of MEA over CeO<sub>2</sub>, the zero-order dependence for both CO<sub>2</sub> pressure and MEA concentration was observed, suggesting that the possible intermediate of CO<sub>2</sub>-captured MEA (*i.e.*, (2-hydroxyethyl)carbamic acid) interacted well with the CeO<sub>2</sub> surfaces. On the other hand, the negative reaction order with respect to CO<sub>2</sub> pressure was found for the CeO<sub>2</sub>-catalyzed conversion of EDA, along with a small dependence on EDA concentration. The inhibitory effect shown by gaseous CO<sub>2</sub> can be explained by a decline in the nucleophilicity of the amino group in the key intermediate of CO<sub>2</sub>-captured EDA (*i.e.*, (2-aminoethyl)carbamic acid) *via* its capping with CO<sub>2</sub>. The DBU-catalyzed reactions of both MEA and EDA were positively dependent on CO<sub>2</sub> pressure and substrate concentration, while the degree of dependence was related to the interaction strength of the plausible intermediate species. In both reactions, the excess CO<sub>2</sub> led to the formation of zwitterionic CO<sub>2</sub>-



captured DBU possessing positive and negative charges at amidine and captured CO<sub>2</sub> moieties, respectively. This DBU-derived species could interact better as a zwitterionic pair with the zwitterionic species derived from EDA and CO<sub>2</sub>, compared to the single anionic species derived from MEA and CO<sub>2</sub>, making the EDA conversion more favorable at higher CO<sub>2</sub> pressure. The kinetic insights into these catalytic reactions with the two different catalysts, CeO<sub>2</sub> and DBU, are precious guidelines for selecting an appropriate catalyst as well as suitable conditions for each target reaction.

## Conflicts of interest

The authors declare no conflicts of interest.

## Data availability

The data supporting this article have been included as part of the supplementary information (SI). Supplementary information is available. See DOI: <https://doi.org/10.1039/d5gc06699a>.

## Acknowledgements

This work was financially supported by the following grants: a Grant-in-Aid for Specially Promoted Research and International Leading Research from the Japan Society for the Promotion of Science (JSPS KAKENHI; grant no. 23H05404 and 23K20034); the ENEOS TonenGeneral Research/Development Encouragement & Scholarship Foundation; and the International Polyurethane Technology Foundation.

## References

- 1 K. Tomishige, M. Tamura and Y. Nakagawa, *Chem. Rec.*, 2019, **19**, 1354–1379.
- 2 X. Zhao, S. Yang, S. Ebrahimiasl, S. Arshadi and A. Hosseinian, *J. CO<sub>2</sub> Util.*, 2019, **33**, 37–45.
- 3 S. Dabral and T. Schaub, *Adv. Synth. Catal.*, 2019, **361**, 223–246.
- 4 K. Tomishige, Y. Gu, Y. Nakagawa and M. Tamura, *Front. Energy Res.*, 2020, **8**, 117.
- 5 H. Li, H. Cheng and F. Zhao, *Asian J. Org. Chem.*, 2022, **11**, e202200338.
- 6 Q.-W. Song, R. Ma, P. Liu, K. Zhang and L.-N. He, *Green Chem.*, 2023, **25**, 6538–6560.
- 7 M. Yabushita, R. Fujii, Y. Nakagawa and K. Tomishige, *ChemCatChem*, 2024, **16**, e202301342.
- 8 K. Takeuchi, *J. Jpn. Pet. Inst.*, 2024, **67**, 45–51.
- 9 K. Tomishige, M. Yabushita and Y. Nakagawa, in *Specialist Periodical Reports – Catalysis*, ed. D. Shekhawat, Royal Society of Chemistry, Cambridge, 2025, vol. 36, pp. 45–90.
- 10 H. Babad and A. G. Zeiler, *Chem. Rev.*, 1973, **73**, 75–91.
- 11 A.-A. G. Shaikh and S. Sivaram, *Chem. Rev.*, 1996, **96**, 951–976.
- 12 B. A. V. Santos, V. M. T. M. Silva, J. M. Loureiro and A. E. Rodrigues, *ChemBioEng Rev.*, 2014, **1**, 214–229.
- 13 M. Honda, M. Tamura, Y. Nakagawa and K. Tomishige, *Catal. Sci. Technol.*, 2014, **4**, 2830–2845.
- 14 M. Tamura, Y. Nakagawa and K. Tomishige, *Asian J. Org. Chem.*, 2022, **11**, e202200445.
- 15 H. Ohno, M. Ikhlayel, M. Tamura, K. Nakao, K. Suzuki, K. Morita, Y. Kato, K. Tomishige and Y. Fukushima, *Green Chem.*, 2021, **23**, 457–469.
- 16 Y. Gu, M. Tamura, Y. Nakagawa, K. Nakao, K. Suzuki and K. Tomishige, *Green Chem.*, 2021, **23**, 5786–5796.
- 17 P. Chen, H. Lin, Y. Kita, K. Nakao, T. Arai, A. Nakayama and M. Tamura, *Energy Fuels*, 2025, **39**, 20506–20516.
- 18 M. Honda, S. Sonehara, H. Yasuda, Y. Nakagawa and K. Tomishige, *Green Chem.*, 2011, **13**, 3406–3413.
- 19 M. Tamura, M. Honda, K. Noro, Y. Nakagawa and K. Tomishige, *J. Catal.*, 2013, **305**, 191–203.
- 20 A. Bansode and A. Urakawa, *ACS Catal.*, 2014, **4**, 3877–3880.
- 21 R. Zhang, L. Guo, C. Chen, J. Chen, A. Chen, X. Zhao, X. Liu, Y. Xiu and Z. Hou, *Catal. Sci. Technol.*, 2015, **5**, 2959–2972.
- 22 D. Stoian, A. Bansode, F. Medina and A. Urakawa, *Catal. Today*, 2017, **283**, 2–10.
- 23 M. Tamura, A. Miura, M. Honda, Y. Gu, Y. Nakagawa and K. Tomishige, *ChemCatChem*, 2018, **10**, 4821–4825.
- 24 D. Stoian, F. Medina and A. Urakawa, *ACS Catal.*, 2018, **8**, 3181–3193.
- 25 Y. Gu, A. Miura, M. Tamura, Y. Nakagawa and K. Tomishige, *ACS Sustainable Chem. Eng.*, 2019, **7**, 16795–16802.
- 26 K. A. Alferov, Z. Fu, S. Ye, D. Han, S. Wang, M. Xiao and Y. Meng, *ACS Sustainable Chem. Eng.*, 2019, **7**, 10708–10715.
- 27 G. S. More and R. Srivastava, *Ind. Eng. Chem. Res.*, 2021, **60**, 12492–12504.
- 28 Y. Gu, M. Tamura, Y. Nakagawa, E. Ando and K. Tomishige, *Catal. Today*, 2023, **410**, 19–35.
- 29 F.-Y. Tu, H.-J. Lai, T.-A. Chiu, J.-C. Jjiang and W.-Y. Yu, *Surf. Interfaces*, 2023, **43**, 103597.
- 30 J.-Y. Chuang, K.-T. Liu, M. M. Lin, W.-Y. Yu, R.-J. Jeng and M. Leung, *J. CO<sub>2</sub> Util.*, 2023, **76**, 102592.
- 31 T. Wei, L. Wang, J. Zhang, Y. Cao, X. Hui, J. Shi, S. Xu, L. Zhao, P. He and H. Li, *Ind. Eng. Chem. Res.*, 2024, **63**, 4338–4352.
- 32 C. Li, C. Che, F. Li, W. Xue, J. Li, X. Zhao and Y. Wang, *Ind. Eng. Chem. Res.*, 2024, **63**, 17757–17766.
- 33 Z. Yang, M. M. Lin, X. Lu, J. T. Zheng, W.-Y. Yu, Y. Zhu, H. Chang and Y. Xia, *Chem. Eng. J.*, 2024, **486**, 150339.
- 34 Z. Yang, J. T. Zheng, X. Lu, M. M. Lin, D. Cai, Y. Wang, W.-Y. Yu, Y. Zhu and Y. Xia, *Mater. Adv.*, 2024, **5**, 6605–6617.
- 35 J. K. Mannisto, J. Heikkinen, J. Puumi, A. Sahari, P. R. Veliz and T. Repo, *Org. Lett.*, 2025, **27**, 5971–5976.
- 36 J. Puumi, A. Sahari, A. Žáková, J. K. Mannisto, N. M. Maier and T. Repo, *ACS Omega*, 2025, **10**, 33843–33849.



- 37 Y. Manaka, Y. Nagatsuka and K. Motokura, *Sci. Rep.*, 2020, **10**, 2834.
- 38 S. Zhang and L. Yan, *ACS Appl. Polym. Mater.*, 2024, **6**, 13350–13358.
- 39 J. A. M. Vargas and A. C. B. Burtoloso, *ChemSusChem*, 2023, **16**, e202300936.
- 40 N. Fanjul-Mosteirín, C. Jehanno, F. Ruipérez, H. Sardon and A. P. Dove, *ACS Sustainable Chem. Eng.*, 2019, **7**, 10633–10640.
- 41 A. W. Kleij, *Curr. Opin. Green Sustainable Chem.*, 2020, **24**, 72–81.
- 42 W. Schilling and S. Das, *ChemSusChem*, 2020, **13**, 6246–6258.
- 43 P.-X. Wu, H.-Y. Cheng, R.-H. Shi, S. Jiang, Q.-F. Wu, C. Zhang, M. Arai and F.-Y. Zhao, *Adv. Synth. Catal.*, 2019, **361**, 317–325.
- 44 E. R. Pérez, M. O. da Silva, V. C. Costa, U. P. Rodrigues-Filho and D. W. Franco, *Tetrahedron Lett.*, 2002, **43**, 4091–4093.
- 45 Z.-Z. Yang, L.-N. He, Y.-N. Zhao, B. Li and B. Yu, *Energy Environ. Sci.*, 2011, **4**, 3971–3975.
- 46 L. Guo, K. J. Lamb and M. North, *Green Chem.*, 2021, **23**, 77–118.
- 47 R. Juárez, P. Concepción, A. Corma and H. García, *Chem. Commun.*, 2010, **46**, 4181–4183.
- 48 M. Tamura, K. Noro, M. Honda, Y. Nakagawa and K. Tomishige, *Green Chem.*, 2013, **15**, 1567–1577.
- 49 A. Primo, E. Aguado and H. Garcia, *ChemCatChem*, 2013, **5**, 1020–1023.
- 50 J. Peng, M. Tamura, M. Yabushita, R. Fujii, Y. Nakagawa and K. Tomishige, *ACS Omega*, 2021, **6**, 27527–27535.
- 51 J. Peng, M. Yabushita, Y. Li, R. Fujii, M. Tamura, Y. Nakagawa and K. Tomishige, *Appl. Catal., A*, 2022, **643**, 118747.
- 52 R. Fujii, M. Yabushita, D. Asada, M. Tamura, Y. Nakagawa, A. Takahashi, A. Nakayama and K. Tomishige, *ACS Catal.*, 2023, **13**, 1562–1573.
- 53 R. Fujii, M. Yabushita, Y. Li, Y. Nakagawa and K. Tomishige, *ACS Catal.*, 2023, **13**, 11041–11056.
- 54 S. Mihara, M. Yabushita, Y. Nakagawa and K. Tomishige, *ChemSusChem*, 2024, **17**, e202301436.
- 55 D. Su, H. Chen, Q. Yang, H. Liu, M. Lv, Y. Zhao, J. Zhou, Q. Zhang, Z. Lu and L. Chen, *J. CO<sub>2</sub> Util.*, 2024, **83**, 102793.
- 56 S. Mihara, N. Mizutani, H. Terada, M. Yabushita, T. Endo, Y. Nakagawa, A. Nakayama and K. Tomishige, *Green Chem.*, 2025, **27**, 14852–14872.
- 57 M. Tamura, M. Honda, Y. Nakagawa and K. Tomishige, *J. Chem. Technol. Biotechnol.*, 2014, **89**, 19–33.
- 58 K. Tomishige, H. Yasuda, Y. Yoshida, M. Nurunnabi, B. Li and K. Kunimori, *Green Chem.*, 2004, **6**, 206–214.
- 59 M. Tamura, R. Kishi, Y. Nakagawa and K. Tomishige, *Nat. Commun.*, 2015, **6**, 8580.
- 60 M. Tamura, R. Kishi, A. Nakayama, Y. Nakagawa, J. Hasegawa and K. Tomishige, *J. Am. Chem. Soc.*, 2017, **139**, 11857–11867.
- 61 T. Chang, M. Yabushita, Y. Nakagawa, N. Fukaya, J.-C. Choi, T. Mishima, S. Matsumoto, S. Hamura and K. Tomishige, *Catal. Sci. Technol.*, 2023, **13**, 5084–5093.
- 62 D. B. Dell'Amico, F. Calderazzo, L. Labella, F. Marchetti and G. Pampaloni, *Chem. Rev.*, 2003, **103**, 3857–3898.
- 63 C. Gouedard, D. Picq, F. Launay and P. L. Carrette, *Int. J. Greenhouse Gas Control*, 2012, **10**, 244–270.
- 64 A. C. Forse and P. J. Milner, *Chem. Sci.*, 2021, **12**, 508–516.
- 65 A. Ion, V. Parvulescu, P. Jacobs and D. De Vos, *Green Chem.*, 2007, **9**, 158–161.
- 66 T. Jiang, X. Ma, Y. Zhou, S. Liang, J. Zhang and B. Han, *Green Chem.*, 2008, **10**, 465–469.
- 67 C. Wu, H. Cheng, R. Liu, Q. Wang, Y. Hao, Y. Yu and F. Zhao, *Green Chem.*, 2010, **12**, 1811–1816.
- 68 M. Marchegiani, M. Nodari, F. Tansini, C. Massera, R. Mancuso, B. Gabriele, M. Costa and N. Della Ca', *J. CO<sub>2</sub> Util.*, 2017, **21**, 553–561.
- 69 H. Koizumi, K. Takeuchi, K. Matsumoto, N. Fukaya, K. Sato, M. Uchida, S. Matsumoto, S. Hamura and J.-C. Choi, *Commun. Chem.*, 2021, **4**, 66.
- 70 X. Zhu, M. Song and Y. Xu, *ACS Sustainable Chem. Eng.*, 2017, **5**, 8192–8198.
- 71 X.-C. Chen, K.-C. Zhao, Y.-Q. Yao, Y. Lu and Y. Liu, *Catal. Sci. Technol.*, 2021, **11**, 7072–7082.
- 72 H. Koizumi, K. Takeuchi, K. Matsumoto, N. Fukaya, K. Sato, M. Uchida, S. Matsumoto, S. Hamura and J.-C. Choi, *ACS Sustainable Chem. Eng.*, 2022, **10**, 5507–5516.
- 73 H. Koizumi, K. Takeuchi, K. Matsumoto, N. Fukaya, K. Sato, M. Uchida, S. Matsumoto, S. Hamura, J. Hirota, M. Nakashige and J.-C. Choi, *J. Org. Chem.*, 2023, **88**, 5015–5024.
- 74 V. Ermatchkov, Á.P.-S. Kamps and G. Maurer, *J. Chem. Thermodyn.*, 2003, **35**, 1277–1289.
- 75 W. Conway, D. Fernandes, Y. Beyad, R. Burns, G. Lawrance, G. Puxty and M. Maeder, *J. Phys. Chem. A*, 2013, **117**, 806–813.
- 76 P. V. Kortunov, L. S. Baugh, M. Siskin and D. C. Calabro, *Energy Fuels*, 2015, **29**, 5967–5989.
- 77 J. K. Mannisto, L. Pavlovic, T. Tiainen, M. Nieger, A. Sahari, K. H. Hopmann and T. Repo, *Catal. Sci. Technol.*, 2021, **11**, 6877–6886.
- 78 X. E. Hu, Q. Yu, F. Barzagli, C. Li, M. Fan, K. A. M. Gasem, X. Zhang, E. Shiko, M. Tian, X. Luo, Z. Zeng, Y. Liu and R. Zhang, *ACS Sustainable Chem. Eng.*, 2020, **8**, 6173–6193.

